HHS Public Access

Author manuscript

Mol Imaging Biol. Author manuscript; available in PMC 2017 August 21.

Published in final edited form as:

Mol Imaging Biol. 2016 December ; 18(6): 820–829. doi:10.1007/s11307-016-0956-7.

A Clinical Wide-Field Fluorescence Endoscopic Device for Molecular Imaging Demonstrating Cathepsin Protease Activity in Colon Cancer

Steven Sensarn[1,2,3], **Cristina L. Zavaleta**[1,3], **Ehud Segal**[4], **Stephan Rogalla**[2], **Wansik Lee**[1,5], **Sanjiv S. Gambhir**[1,3,6,7], **Matthew Bogyo**[4], and **Christopher H. Contag**[1,2,3,8,9]

[1]Department of Radiology, Stanford University, James H. Clark Center for Biomedical Engineering & Sciences, Stanford, CA, 94305, USA

[2]Department of Pediatrics, Stanford University, James H. Clark Center for Biomedical Engineering & Sciences, Stanford, CA, 94305, USA

[3]Molecular Imaging Program at Stanford (MIPS), Stanford University, Stanford, CA, 94305, USA

[4]Department of Pathology, Stanford University, Stanford, CA, 94305, USA

[5]Department of Internal Medicine, Chonnam National University Medical School, Gwangju, Republic of Korea

[6]Department of Bioengineering, Stanford University, Stanford, CA, 94305, USA

[7]Department of Materials Science and Engineering, Stanford University, Stanford, CA, 94305, USA

[8]Department of Microbiology & Immunology, Stanford University, Stanford, CA, 94305, USA

[9]Stanford University, 318 Campus Drive, Stanford, CA, 94305-5427, USA

Abstract

Purpose—Early and effective detection of cancers of the gastrointestinal tract will require novel molecular probes and advances in instrumentation that can reveal functional changes in dysplastic and malignant tissues. Here, we describe adaptation of a wide-field clinical fiberscope to perform wide-field fluorescence imaging while preserving its white-light capability for the purpose of providing wide-field fluorescence imaging capability to point-of-care microscopes.

Procedures—We developed and used a fluorescent fiberscope to detect signals from a quenched probe, BMV109, that becomes fluorescent when cleaved by, and covalently bound to, active

Correspondence to: Christopher Contag; ccontag@stanford.edu.
Steven Sensarn and Cristina L. Zavaleta contributed equally to this work.

Electronic supplementary material The online version of this article (doi:10.1007/s11307-016-0956-7) contains supplementary material, which is available to authorized users.

Compliance with Ethical Standards

Conflict of Interest

The authors declare that they have no conflict of interest.

Ethical Approval

All applicable institutional and/or national guidelines for the care and use of animals were followed.

cathepsin proteases. Cathepsins are expressed in inflammation- and tumor-associated macrophages as well as directly from tumor cells and are a promising target for cancer imaging. The fiberscope has a 1-mm outer diameter enabling validation via endoscopic exams in mice, and therefore we evaluated topically applied BMV109 for the ability to detect colon polyps in an azoxymethane-induced colon tumor model in mice.

Results—This wide-field endoscopic imaging device revealed consistent and clear fluorescence signals from BMV109 that specifically localized to the polypoid regions as opposed to the normal adjacent colon tissue ($p < 0.004$) in the murine colon carcinoma model.

Conclusions—The sensitivity of detection of BMV109 with the fluorescence fiberscope suggested utility of these tools for early detection at hard-to-reach sites. The fiberscope was designed to be used in conjunction with miniature, endoscope-compatible fluorescence microscopes for dual wide-field and microscopic cancer detection.

Keywords

Optical imaging; Optical probes; Endoscopy; Fluorescence; Imaging systems; Medical imaging; Fiber optics; Biomedical optics

Introduction

Cancer remains the second most common cause of death in the USA, with over 1.6 million new cancer cases estimated this year according to the American Cancer Society [1]. Even more alarming is the 585,000 cancer-related deaths expected this year in the US alone. Diagnostic tools that enable early detection, including endoscopy as a screening procedure for colon cancer, have been shown to reduce cancer mortality [2–4]. However, many of the imaging tools available for clinical screening, including endoscopy, are limited by the use of white light revealing gross structural abnormalities based on visual inspection. As such, white-light endoscopy has miss rates of up to 25 % [5]. Therefore, the development of point-of-care diagnostic tools that offer additional molecular information with sufficient sensitivity and specificity for early cancer detection is critical for effective early detection and early intervention. Toward this end, fluorescence endoscopy has the potential for sensitive molecular analyses through the use of fluorescent molecular probes that have specificity for dysplastic or malignant tissues [6–13]. To effectively detect such functional probes, new accessories that image over a range of scales from macro- to microscopic levels and are compatible with clinical endoscopes need to be developed. Effective optical tools with a breadth of capabilities would facilitate cancer detection and have the potential to significantly impact the survival rates of patients.

Mouse models are typically used for development of molecular probes, and a number of instruments have been described that enable molecular detection of colon cancer in mice [14–18]. Endoscope design options for colonoscopy in mice are limited to a device diameter less than approximately 3.5 mm [19]. Rigid borescopes yield beautiful, high-resolution [20] rodent endoscopic images but have limited length and cannot navigate beyond the distal colon, restricting their utility. Fiber bundle-based endoscopes—fiberscopes—may have poorer resolution than rigid scopes but have a much smaller cross section (≤1 mm), ease of

sterilization, and simplicity of manufacture, and may serve as an adjunct modality for other high-resolution imaging tools. Fiberscopes are particularly well suited for fluorescence imaging since they can be made very small, use extremely sensitive detectors, such as intensified or electron-multiplying cameras, and can detect weak fluorescence signals through the working channels of existing clinical endoscopes [21]. Also, when used in conjunction with targeted molecular probes, the resolution of a fiberscope is less prohibitive and can reveal the presence of fluorescence signals—rather than relying on high-resolution morphological detail, and may be sufficient to guide further inspection with more high-resolution devices that have smaller fields of view, or to guide biopsy. Fluorescence-enabled fiberscopes would have utility in animal models, and would also be suitable for use with clinical devices for early detection, guided microscopy and image-guided biopsy.

Here, we describe modifications to a commercially available white-light fiberscope for use as a wide-field fluorescence endoscope, and demonstrate its use in mouse models. The fiberscope is currently approved by the Food and Drug Administration (FDA) for white-light imaging of bile ducts and can be sterilized and reused, making it a promising candidate for adding small-footprint fluorescence imaging to endoscopic devices in the clinic and for incorporation into other devices to create multifunctional instruments that operate over a range of scales using several different modes. In addition to its clear clinical applications, this device also has potential for use as a preclinical imaging device to assess the tumor-targeting efficiency of newly developed optical probes, in preparation for clinical translation.

We have adapted the 1-mm fiberscope to perform dual white-light and fluorescence imaging, and demonstrated its use in the distal colon of mice where we were able to evaluate the location, shape, and size of polyps. This is particularly useful when planning experiments in expensive transgenic mouse models and time-intensive carcinogen-induced models. No other preclinical imaging technique currently exists to assess tumor progression in orthotopic colon cancer models in real time, and therefore time and materials are often wasted in the testing of new drugs or tumor-targeting agents. We demonstrate functional imaging using BMV109, a fluorescent probe designed to target active cathepsin proteases expressed by inflammation- and tumor-associated macrophages and certain tumor cells themselves [22]. The probe has similar pan-cathepsin-targeting activity as the previously described MV151 [23] but utilizes a quencher that is cleaved upon activation, such that the probe is activated at the tumor site. Used in conjunction with an azoxymethane-induced (AOM) mouse model of colon cancer, the device and molecular probe demonstrated sensitive and specific targeting of colorectal tumors. We revealed that the combination of the wide-field fluorescence fiberscope and the cathepsin-activated probe reliably detected small polyps in relevant rodent models indicating utility in early detection of human disease.

Material and Methods

Small Animal Fluorescence Endoscope

The core component of the endoscope used in this study is the SpyGlass fiber-optic probe from Boston Scientific. The device is FDA-approved for white-light cholangiography and consists of a 6600-fiber imaging bundle surrounded by 225 wide-angle illumination fibers. The probe has an outer diameter of less than 1 mm and images a 70-degree field of view. We

have adapted the fiberscope to perform dual white-light and fluorescence imaging utilizing a dual-illumination setup with a laser and light-emitting diode (LED), as well as a removable mirror detection scheme.

For illumination, a 660-nm fiber-coupled diode laser (Coherent CUBE) was coupled into the SpyGlass light guide port using a 60× aspheric lens. A white-light LED placed beside the laser beam is used for white-light endoscopy. Controlled by remote switches, the laser and LED produce approximately 3 and 0.3 mW of light, respectively, measured at the output of the SpyGlass. For detection, a 20× microscope objective images the output from the fiber bundle onto one of two CCD cameras: a sensitive EMCCD camera for fluorescence (Andor Luca S) or a color CCD camera for white-light imaging (Hitachi KP-D20B). Inserting or removing a 45-degree mirror selects the desired camera. A long-pass interference filter with an edge wavelength of 664 nm is used in conjunction with a lens tube system to filter out background light—from the laser, environment, and fluorescence generated from the illumination fibers—before it reaches the EMCCD camera. The digital images from the EMCCD camera are recorded directly to disk at 24 frames per second, while the analog NTSC signal from the color camera is hardware-encoded to an MPEG-2 video using a USB capture cable (StarTech SVID2USB2NS).

For *in vivo* imaging, the modified fiberscope was introduced into the distal colon of mice using a flexible endoscope made from thin-wall plastic tubing (1.8-mm diameter). The tubing was glued to a catheter Y connector enabling the fiberscope to pass through with an airtight seal. The second input of the Y connector was connected to an air source for insufflation of the colon. The air source consists of an air pump followed by a pressure regulator and gang valves used to adjust output pressure and airflow (measured using a water column manometer). Before each procedure, the airflow system was adjusted to produce a maximum pressure of 6 mmHg in the colon, below the minimum pressure used in a colorectal distension sensitivity study in C57BL/6 J mice [24].

The fluorescence endoscopy system utilizes a portable cart containing all of the necessary hardware. Figure 1 shows the cart, optics, and endoscope prior to a mouse colonoscopy procedure.

Video and Image Processing

Full image frames from the EMCCD camera were directly spooled to the hard drive in chunks using the Andor SOLIS software. Individual 16-bit grayscale images were extracted from the chunks in PNG format using the ImageMagick software. The MATLAB software was used to preprocess the raw images, performing 2 × 2 binning and encoding the 16-bit grayscale images as 24-bit color RGB images supported by the AviSynth frameserving software (by storing the most significant and least significant bytes into the red and green channels, respectively). The AviSynth was used, with a custom plug-in, to contrast scale the images from the encoded 24-bit RGB format to 8-bit grayscale for display on computer monitors. The AviSynth script was also used to combine and synchronize fluorescence video frames with white-light frames from the color CCD camera and to blur images to reduce pixilation arising from the small gaps between fibers in the fiberscope. The MeGUI software was used in conjunction with the AviSynth script to encode frames into video.

Fiberscope Sensitivity and Resolution Measurement

The sensitivity of the fiberscope system was measured using a 96-well plate (Neuro Probe 101-5) with 30-μl capacity, 3.2-mm diameter wells filled with various amounts of Cy5 (the fluorophore component of BMV109). A half logarithmic dilution series was used to test Cy5 quantities ranging from 10 pmol to 10 fmol in 20 μl volumes of dimethylformamide (DMF). A cardboard box with the bottom cut out and a small hole on top was placed over the well plate, and the fiberscope was fed through the hole and fixed about 3 mm above the well plate. The box was then shifted to move the fiberscope from well to well as fluorescence image frames were acquired. As described in "Video and Image Processing," the raw images were preprocessed into 24-bit RGB-encoded format, and a single frame (41.67 ms acquisition time) was chosen from each well for signal quantification in the MATLAB. Mean pixel values within a circular region of interest (ROI) surrounding the Cy5 solution were calculated from the images and plotted against Cy5 quantity to estimate the detection limit. After imaging each well on the plate, the measurements were repeated a second time.

To determine resolution, a vinyl laminate test pattern (1951 USAF test pattern, Edmund Optics) was illuminated with an external LED light source and imaged with the fiberscope in white-light mode. The fiberscope was brought very close to the test pattern to best resolve the smallest elements, as determined visually. The AviSynth was used to reduce pixilation from the fibers as mentioned in "Video and Image Processing."

Mouse Colonoscopy

Colon tumors were induced in A/J mice by weekly intraperitoneal injections of 1 mg/kg azoxymethane for 6 weeks, beginning at 6–8 weeks of age. By about 6 months after treatment, the mice developed numerous tumors with a range of sizes in the distal colon. The size, shape, and location of some of the polyps were confirmed visually with the white-light imaging function of our fiberscope before administration of our fluorescent "smart" probe. Multiple polypoid tumors in three mice, with a range of sizes, were examined in our studies to demonstrate targeted fluorescence imaging of cathepsins in tumors.

Prior to imaging, mice were anesthetized with 2 % isoflurane through a nose cone and placed in the supine position on a heated surgery pad. A 24G Abbocath-T catheter and syringe were used to administer PBS enemas to clear feces from the distal colon prior to administration of BMV109. Another 24G catheter was used to administer BMV109 probe (200 μl, 10 μmol BMV109 in 10 % DMSO, 30 % ethanol, and 60 % PBS) intrarectally, while the anus was pinched by hand and slightly elevated. After a few minutes, the pinching was discontinued, and the catheter left inside the rectum while the probe incubated in the colon for 45 min.

After incubation, two PBS enemas were administered to wash out unbound probe. To demonstrate *in vivo* imaging, the endoscope was coated with a small amount of Aquagel lubricant and carefully introduced into the rectum. While one operator slowly inserted and retracted the endoscope within the colon, the other switched the laser and LED on and off and removed/replaced the removable mirror on the optics breadboard to switch between white-light and fluorescence imaging modes.

Ex Vivo Imaging

To simulate the human use case, where the fiberscope would be aimed directly at the colon wall in close proximity, and to allow imaging of polyps proximal to the splenic flexure (unreachable by our endoscope *in vivo*), the mice were sacrificed and their colons removed, excised tissues were rinsed in PBS, and cut open and placed on black paper for *ex vivo* imaging. The fiberscope was mounted in a cardboard box as described in "Fiberscope Sensitivity and Resolution Measurement" and scanned over the tissue surface in fluorescence imaging mode. A commercial wide-field fluorescence imaging device (Xenogen IVIS 200, Perkin Elmer) was also used to produce high-resolution images of the colon tissue and confirm contrast observed with the fiberscope.

Image and Statistical Analysis

The open source ImageJ image analysis software was used to draw regions of interest within the fluorescent images acquired with our fiberscope. Within each mouse ($n = 3$), three separate polyps were identified and analyzed for fluorescence signal intensity and compared with three separate normal adjacent regions within the colon of each mouse. A student's t test was used to compare fluorescence signal intensity acquired from our fiberscope between the colon polyps and the normal adjacent colon tissue. An equality of variances test was performed and revealed little variance between the groups. Therefore, a one-tailed t test assuming equal variances was performed to determine statistical significance because it was hypothesized that the colon polyps would have greater localized fluorescence signal with little to no activation in the surrounding normal adjacent colon tissue. The values reported appear as mean ± standard error of mean (SEM).

Dual-Axis Confocal Microscopy of Colon Polyps

To confirm cellular activation of BMV109 in colon polyps and to rule out non-specific contrast (e.g., adhesion to the mucus layer of polyps), a fourth mouse (similar to those described in "Mouse Colonoscopy" but a C57BL/6 strain with polyps induced by both azoxymethane and dextran sodium sulfate) was treated and imaged as before, with the colon removed and placed on black paper. After fiberscope imaging, however, fluorescent polyps were excised and imaged using a dual-axis confocal (DAC) microscope [25]. The confocal microscope produces an image stack of optical sections from thick tissue samples without the need for physical sectioning or processing. This stack can be rendered in 3D to visualize the tissue morphology at the cellular level. By holding the photomultiplier tube gain constant between samples, the relative fluorescence levels can be compared.

Results

Fiberscope Sensitivity and Resolution

Figure 2a shows fluorescence images from Cy5 dilutions in a well plate. A negative control well contained pure DMF. All images are contrast scaled equally for visual comparison, resulting in the higher concentrations appearing saturated. Signals were not scaled or truncated for quantitation (Fig. 2b). Average pixel values computed within the yellow ROIs are plotted in Fig. 2b, along with a linear fit (solid line) and its y intercept (dashed line,

representing the background level). The DMSO control is plotted as 1 fmol to fit on the logarithmic *x* axis. The fiberscope was able to clearly detect 316 fmol of Cy5 within the 41.67-ms acquisition, and a trained operator may be able to identify levels as low as 100 fmol (visible just above background).

Figure 2c shows the resolution of the fiberscope. Group 3, element 1 of the 1951 USAF resolution test pattern is clearly resolved, demonstrating the ability to distinguish eight line pairs/millimeter, or a line thickness of 62.5 μm.

Detection of BMV109 in Colon Polyps of Mice

In vivo imaging of a large colon polyp is shown in Fig. 3. The system was switched from white-light to fluorescence imaging mode in about 7 s. Localization of BMV109 to the polyp is visible in fluorescence (Fig. 3b). Video 1 shows both white-light and fluorescence imaging of the polyp after processing, with the white-light camera displayed on the left half of the video and the fluorescence EMCCD camera on the right half (see “Video and Image Processing”). During the procedure, the live camera views were displayed on separate monitors simultaneously, demonstrating the clinical use case. To access more polyps with a range of sizes and to demonstrate a more clinically applicable tissue-surveying technique (pointing the fiberscope directly at the colon wall), *ex vivo* fluorescence imaging was performed on colons from the three mice. Figure 4a and Video 2 show results from mouse M1. In the color camera photo, the entire colon is visible (distal end to the left). The white square in the image indicates the approximate region of tissue that was scanned in Video 2. The white circle indicates the field of view shown in the fluorescence fiberscope image to the right of Fig. 4a. Fluorescence contrast was observed in polyps against a dark background of normal tissue. Figure 4b shows the results from mouse M2 (the same mouse used for *in vivo* imaging in Fig. 3). In addition to the color camera photo and fiberscope image, an IVIS 200 fluorescence image is included (bottom left). The ruler to the left of the image indicates tissue dimensions with a minor tick spacing of 2 mm. The fluorescence contrast observed in the fiberscope frame of Fig. 4b and Video 3 are confirmed by the IVIS 200 image. Finally, Fig. 4c and Video 4 show the same three modalities (color camera, fiberscope fluorescence, and IVIS 200 fluorescence) for mouse M3. The graph in Fig. 4d reveals a significant difference in fluorescence intensity between the colon polyps and the normal adjacent tissue within three different tumor-bearing mice. Regions of interest were drawn within the fluorescent images acquired from our fiberscope to determine relative fluorescence signal intensity. Three separate regions were drawn around three separate polyps and compared to three separate surrounding normal areas within each colon of the tumor-bearing mice ($n = 3$).

There is a range of both small and large polyps that appeared to be at different stages of growth, including lesions approximately 2 mm in size (Fig. 4b, c). Lesions 2 mm and below can be difficult to visualize with conventional colonoscopy, particularly by less-experienced clinicians or with imperfect preparation of the colon [32]. Our results show high tumor to background signal and demonstrate that the wide-field fluorescence endoscope is able to detect differences in signal intensity offering both sensitivity and specificity.

Dual-Axis Confocal Images Confirm Cellular Uptake in Polyps

Fluorescence from BMV109 was confirmed by wide-field imaging (Fig. 5e and Video 5), and DAC microscope images indicated cellular uptake in excised polyps from mouse M4. Three-dimensional-rendered DAC images of polyps (Fig. 5a–c) show strong, localized fluorescence signal in cells, with the exception of the polyp in Fig. 5a, which also exhibited weak fluorescence by fiberscope. Images from randomly selected adjacent normal mucosa (Fig. 5d) contain minimal fluorescence signal and correspond to the dark regions surrounding the polyps in Video 5. The DAC configuration is amenable to miniaturization [25–28] and was used here to demonstrate the utility of using a miniaturized DAC in conjunction with the fluorescence-adapted fiberscope for a combination of a wide-field finder scope and a miniature microscope for macroscopic and microscopic detection of cancers at epithelial surfaces.

Discussion

If we are to decrease the numbers of epithelial cancer-related deaths, we need to develop effective tools for early detection of dysplastic or malignant neoplasia such that intervention can be initiated when the disease can still be controlled. Since the luminal surface of the colon is an accessible tissue, white-light endoscopy has revolutionized the way we evaluate colorectal cancer resulting in significant decreases in cancer incidence and mortality. From this, we reasoned that we could build on this current standard of care and improve early detection with more advanced visualization tools [2–4]. Even in a powerful diagnostic approach such as endoscopy, neoplastic lesions can still be missed, particularly polyps less than 5 mm in size and flat lesions that can potentially progress into invasive carcinoma [29–33]. Additionally, the current gold standard of removing virtually all visualized polyps followed by histology leads to excess polypectomies and histology costs since more than half of all resected polyps are non-neoplastic [34, 35]. An accessory tool that allows for real-time in vivo classification of neoplastic lesions could significantly improve early cancer detection and thus patient outcome.

As a result, significant effort has been focused on developing better endoscopic accessory tools to enhance colorectal cancer detection. Some of the optically based endoscopic imaging techniques include narrow-band imaging, magnifying endoscopy, light scattering spectroscopy, autofluorescence imaging, optical coherence tomography, chromoendoscopy, and confocal microendoscopy [5, 36–41]. Most of these technologies rely on visually assessing surface structure to determine demarcation borders, and highlighting mucosal details such as capillary and pit patterns on the colon wall, providing little or no functional information. Some techniques look at basic tissue architecture through fluorescence, or characterizing crevices and concave areas with the use of chromogenic dyes, while other techniques focus on microanatomic changes between normal and dysplastic lesions [37, 40, 42].

Video capsule endoscopy which uses ingestible capsules for diagnosis of gastrointestinal disease is another up and coming imaging technology that predominantly looks at structural details but has the potential to look at molecular details [43]. Current versions have color enhancement options that offer variable wavelength settings, which could be used for optical

probe detection. However, at present, image interpretation can be very time consuming, since up to 50,000 images can be generated during video capsule endoscopy. New software is currently being developed to reduce the time needed to interpret the images from 5 h to 1 h [44]; however, this could lead to increased miss rates.

The ability to visualize disease-specific molecular changes beyond structural differences in glandular or nuclear morphology can increase the efficacy of endoscopic screening for improved diagnosis. The importance of functional information to guide endoscopy has been noted by other investigators, and molecularly targeted fluorescent probes have been tested in both mouse models and humans [6, 9, 15, 41, 42, 45–47]. Fluorescence endoscopy can play an important role, because several tumor-targeting molecular probes like peptides, antibodies, activated probes, and nanoparticles can be conjugated with fluorescent dyes and localized using a fluorescence endoscope.

Devices with high resolution, such as endomicroscopes, i.e., Cellvizio (Mauna Kea Technologies), have excellent resolution but are limited to small fields of view such that only a small predetermined area of interest can be examined and are thus inappropriate for surveying large areas quickly. Our wide-field fluorescence device is a complementary accessory for these endomicroscopes as well as white-light endoscopy, because our fluorescence-adapted fiberscope has the capability of surveying large areas in real time to guide microscopic imaging of a particular area of interest.

The fluorescence fiberscope can be adapted for imaging of molecular probes over a wide range of excitation and emission wavelengths. The 660-nm fiber-coupled diode laser was specifically chosen in this study for optimal excitation of the cathepsin-activated probe, BMV109, that bears a Cy5 fluorescent tag. However, any number of near infrared, or tunable, lasers may be used including those with longer wavelengths with greater light penetration into tissues due to less hemoglobin absorption, and modest autofluorescence.

The fluorescence from polyps was not necessarily uniform from polyp to polyp—this has been addressed in prior publications on BMV109 and related molecular probes [47]. Previous studies have demonstrated an imperfect correlation between polyp size and fluorescence, as well as bound fluorescence for various cathepsins expressed by polyps [47]. To summarize their findings, the amount of fluorescence generated by the activated probe depends on the tumor genotype and cathepsin expression of the polyps as well as their raw size (with larger polyps generally containing more proteases and higher fluorescence).

Molecular targeting can be achieved utilizing highly specific molecular probes with high binding affinities. Bioconjugation of such probes with fluorescent dyes or nanoparticles has been used to target biomarkers that are overexpressed in colon cancers such as c-Met, VEGF, EGFR, or metalloproteinases [6, 9, 48–51]. The highly specific binding affinity provides an increased signal-to-noise ratio resulting in a visual contrast of the neoplastic lesion against the normal mucosal background. A significant problem with *in vivo* fluorescence imaging is the background due to the inability to effectively wash off unbound probe. To reduce this source of noise, we utilized a “smart” activated probe in which there is only signal after interaction with the target enzyme. The advantage of these probes is that

they only fluoresce after they have been cleaved by tumor-associated proteases, virtually eliminating non-specific fluorescent background signal. The fluorescence activity of these molecular beacons is quenched in their native state but becomes fluorescent when covalently bound to, and cleaved by, active proteases (i.e., cathepsins) [12, 47] expressed by the tumor cells and tumor-associated macrophages.

When considering clinical translation of an intrarectal dosing approach, it is important to clear the mucosal layer within the colon because it can act as a barrier for our molecular probe to reach its intended target on the epithelial wall. While the technique of utilizing an intrarectal enema of a DMSO/ethanol cocktail as a mucolytic is not ideal for clinical translation, there are alternative strategies that are currently being used in the clinic for clearing the thick mucosal layer like the administration of acetic acid (vinegar) [52]. It is important to note that the BMV109 probe is still under development, and that other administration approaches are currently being investigated that may be better suited for clinical translation [47]. However, if this probe were to be administered topically to the colon, one could envision an enema that could be mixed with a small percentage of acetic acid to help clear the mucosal layer. An enema could be administered prior to routine colonoscopy and allowed to incubate for a given period of time followed by a rinse with water to clear the unbound probe. The routine white-light colonoscopy could then commence while using our accessory wide-field endoscopic tool to help guide the physician and provide a molecular map of the targeted optical imaging probe to improve real-time detection of dysplastic and cancerous lesions. It is important to note that although different optical probes may be used to enhance the specificity, our newly developed wide-field fluorescence endoscope has shown to be very sensitive in detecting the BMV109 probe in this study. Our endoscope has been designed to fit into the accessory channel of most conventional endoscopes without perturbing its routine white-light functions in the clinic.

Although our wide-field device was developed for the clinic and for use in combination with other imaging tools, its small size also offers the ability to be tested in small laboratory animal models, and may find utility for advancing the study of rodent models of gastrointestinal cancers. The small size allowed us to assess its utility with cathepsin probes in rodent models, and will enable testing of various new investigational molecular probes, and the device design was intentional such that it, and the probe, can then be translated to the clinic without the need for a translational bridge between basic and clinical sciences.

It is important to stress that although we initially focused our efforts on improving colon cancer detection, our newly developed wide-field molecular imaging device could be easily deployed through the accessory channel of many clinical endoscopes/rigid borescopes that already utilize white-light endoscopy. Tissues that already utilize clinical endoscopy for cancer diagnosis include the bladder, stomach, esophagus, lungs, cervix, and skin. Intraoperative strategies could also benefit greatly from our newly developed molecular imaging device, which could aid surgeons in identifying tumor margins in real time while potentially improving tumor resection.

Conclusion

We have adapted a commercially available clinical fiberscope to perform wide-field fluorescence imaging in addition to its present white-light capability. This will have potential for detecting molecular probes in difficult to reach areas of the body. In conjunction with a custom-made colonoscope, the wide-field fluorescent system was able to identify fluorescence from a topically applied molecular probe in colon polyps of carcinogen-treated mice. These results confirm that the fiberscope has the sensitivity to detect emission from fluorescent probes localized to polyps with a high signal-to-noise ratio. The primary sources of targeted cathepsins are macrophages that migrate to and infiltrate the tumor sites. Using a miniaturized DAC microscope, we have confirmed cellular uptake of BMV109 in tumor epithelium, suggesting lysosomal uptake, cleavage, and binding of the activated molecule. Because macrophages are present both in cancer and inflammation, the combination of BMV109 and miniature fluorescence imaging tools has potential for detecting early disease. The small cross section of the SpyGlass makes it easy to incorporate with existing endoscopic tools, such as our miniature DAC microscopes or the Mauna Kea Cellvisio, enabling dual wide-field white-light and fluorescence imaging with high-resolution microscopy for point-of-care pathology. This clinical fiberscope has sufficient resolution to guide miniature fluorescence microscopes for *in vivo* optical pathology, and we envision combined fiberscope/microscope devices used for point-of-care optical pathology and guided resection during routine cancer screening.

Acknowledgments

The authors thank the Stanford Small Animal Imaging Facility for resources and technical support. We would also like to thank Pankaj Pasricha, Martijn Verdoes, Laura Edgington, James Amos-Landgraff, Laura Bronsart, Bonnie King, and the laboratory of Lawrence Marnett for equipment, assistance, and discussions aiding in the development of our imaging system. This work was supported in part by the National Cancer Institute (U54 CA136465 and P50 CA114747), the Canary Foundation, and a generous gift from the Chambers Family Foundation for Excellence in Pediatric Research. Steven Sensarn was supported by the Stanford Cancer Imaging Training fellowship from the NCI (5 T32 CA 9695-19). Cristina Zavaleta was supported by the National Cancer Institute of the National Institutes of Health under Award Number K22 CA160834.

References

1. American Cancer Society. [Accessed 17 Feb 2015] Cancer Facts and Figures. 2014. http://www.cancer.org/research/cancerfactsstatistics/cancerfactsfigures2014
2. Vital signs. Colorectal cancer screening, incidence, and mortality—United States, 2002–2010. MMWR Morb Mortal Wkly Rep. 2011:884–889. [PubMed: 21734636]
3. Winawer SJ, Zauber AG, Ho MN, et al. Prevention of colorectal cancer by colonoscopic polypectomy. The National Polyp Study Workgroup. N Engl J Med. 1993; 329:1977–1981. [PubMed: 8247072]
4. Zauber AG, Winawer SJ, O'Brien MJ, et al. Colonoscopic polypectomy and long-term prevention of colorectal-cancer deaths. N Engl J Med. 2012; 366:687–696. [PubMed: 22356322]
5. Stallmach A, Schmidt C, Watson A, Kiesslich R. An unmet medical need: advances in endoscopic imaging of colorectal neoplasia. J Biophotonics. 2011; 4:482–489. [PubMed: 21674811]
6. Barrett T, Koyama Y, Hama Y, et al. In vivo diagnosis of epidermal growth factor receptor expression using molecular imaging with a cocktail of optically labeled monoclonal antibodies. Clin Cancer Res. 2007; 13:6639–6648. [PubMed: 17982120]

7. Fujii T, Kamiya M, Urano Y. In vivo imaging of intraperitoneally disseminated tumors in model mice by using activatable fluorescent small-molecular probes for activity of cathepsins. Bioconjug Chem. 2014; 25:1838–1846. [PubMed: 25196809]
8. Kim SY, Myung SJ. Optical molecular imaging for diagnosing intestinal diseases. Clin Endosc. 2013; 46:620–626. [PubMed: 24340254]
9. Oh G, Yoo SW, Jung Y, et al. Intravital imaging of mouse colonic adenoma using MMP-based molecular probes with multi-channel fluorescence endoscopy. Biomed Opt Express. 2014; 5:1677–1689. [PubMed: 24877024]
10. Urano Y, Asanuma D, Hama Y, et al. Selective molecular imaging of viable cancer cells with pH-activatable fluorescence probes. Nat Med. 2009; 15:104–109. [PubMed: 19029979]
11. Verdoes M, Edgington LE, Scheeren FA, et al. A nonpeptidic cathepsin S activity-based probe for noninvasive optical imaging of tumor-associated macrophages. Chem Biol. 2012; 19:619–628. [PubMed: 22633413]
12. Verdoes M, Oresic Bender K, Segal E, et al. Improved quenched fluorescent probe for imaging of cysteine cathepsin activity. J Am Chem Soc. 2013; 135:14726–14730. [PubMed: 23971698]
13. Gounaris E, Martin J, Ishihara Y, et al. Fluorescence endoscopy of cathepsin activity discriminates dysplasia from colitis. Inflamm Bowel Dis. 2013; 19:1339–1345. [PubMed: 23591598]
14. Funovics MA, Alencar H, Su HS, et al. Miniaturized multichannel near infrared endoscope for mouse imaging. Mol Imaging. 2003; 2:350–357. [PubMed: 14717334]
15. Funovics MA, Alencar H, Montet X, et al. Simultaneous fluorescence imaging of protease expression and vascularity during murine colonoscopy for colonic lesion characterization. Gastrointest Endosc. 2006; 64:589–597. [PubMed: 16996355]
16. Miller SJ, Joshi BP, Feng Y, et al. In vivo fluorescence-based endoscopic detection of colon dysplasia in the mouse using a novel peptide probe. PLoS One. 2011; 6:e17384. [PubMed: 21408169]
17. Liu Z, Miller SJ, Joshi BP, Wang TD. In vivo targeting of colonic dysplasia on fluorescence endoscopy with near-infrared octapeptide. Gut. 2013; 62:395–403. [PubMed: 22427239]
18. Miller SJ, Lee CM, Joshi BP, Gaustad A, Seibel EJ, Wang TD. Targeted detection of murine colonic dysplasia in vivo with flexible multispectral scanning fiber endoscopy. J Biomed Opt. 2012; 17:021103. [PubMed: 22463021]
19. Becker C, Fantini MC, Neurath MF. High resolution colonoscopy in live mice. Nat Protoc. 2006; 1:2900–2904. [PubMed: 17406549]
20. Becker C, Fantini MC, Wirtz S, et al. In vivo imaging of colitis and colon cancer development in mice using high resolution chromoendoscopy. Gut. 2005; 54:950–954. [PubMed: 15951540]
21. Ogihara T, Watanabe H, Namihisa A, et al. Clinical experience using a real time autofluorescence endoscopy system in the gastrointestinal tract. Diagn Ther Endosc. 1999; 5:119–124. [PubMed: 18493491]
22. Mohamed MM, Sloane BF. Cysteine cathepsins: multifunctional enzymes in cancer. Nat Rev Cancer. 2006; 6:764–775. [PubMed: 16990854]
23. Verdoes M, Florea BI, Menendez-Benito V, et al. A fluorescent broad-spectrum proteasome inhibitor for labeling proteasomes in vitro and in vivo. Chem Biol. 2006; 13:1217–1226. [PubMed: 17114003]
24. Larsson M, Arvidsson S, Ekman C, Bayati A. A model for chronic quantitative studies of colorectal sensitivity using balloon distension in conscious mice—effects of opioid receptor agonists. Neurogastroenterol Motil. 2003; 15:371–381. [PubMed: 12846725]
25. Wang TD, Contag CH, Mandella MJ, et al. Confocal fluorescence microscope with dual-axis architecture and biaxial postobjective scanning. J Biomed Opt. 2004; 9:735–742. [PubMed: 15250760]
26. Wang D, Chen Y, Leigh SY, et al. Microscopic delineation of medulloblastoma margins in a transgenic mouse model using a topically applied VEGFR-1 probe. Translat Oncol. 2012; 5:408–414.
27. Ra H, Piyawattanametha W, Gonzalez-Gonzalez E, et al. In vivo imaging of human and mouse skin with a handheld dual-axis confocal fluorescence microscope. J Invest Dermatol. 2011; 131:1061–1066. [PubMed: 21191407]

28. Wang TD, Mandella MJ, Contag CH, Kino GS. Dual-axis confocal microscope for high-resolution in vivo imaging. Opt Lett. 2003; 28:414–416. [PubMed: 12659264]
29. Leggett B, Whitehall V. Role of the serrated pathway in colorectal cancer pathogenesis. Gastroenterology. 2010; 138:2088–2100. [PubMed: 20420948]
30. Nawa T, Kato J, Kawamoto H, et al. Differences between right-and left-sided colon cancer in patient characteristics, cancer morphology and histology. J Gastroenterol Hepatol. 2008; 23:418–423. [PubMed: 17532785]
31. Okamoto M, Kawabe T, Yamaji Y, et al. Flat-type early colorectal cancer preferentially develops in right-sided colon in older patients. Dis Colon Rectum. 2005; 48:101–107. [PubMed: 15690665]
32. Soetikno RM, Kaltenbach T, Rouse RV, et al. Prevalence of nonpolypoid (flat and depressed) colorectal neoplasms in asymptomatic and symptomatic adults. J Am Med Assoc. 2008; 299:1027–1035.
33. Torlakovic E, Skovlund E, Snover DC, et al. Morphologic reappraisal of serrated colorectal polyps. Am J Surg Pathol. 2003; 27:65–81. [PubMed: 12502929]
34. Diamond SJ, Enestvedt BK, Jiang Z, et al. Adenoma detection rate increases with each decade of life after 50 years of age. Gastrointest Endosc. 2011; 74:135–140. [PubMed: 21612774]
35. Huang CS, O'Brien MJ, Yang S, Farraye FA. Hyperplastic polyps, serrated adenomas, and the serrated polyp neoplasia pathway. Am J Gastroenterol. 2004; 99:2242–2255. [PubMed: 15555008]
36. Dacosta RS, Wilson BC, Marcon NE. New optical technologies for earlier endoscopic diagnosis of premalignant gastrointestinal lesions. J Gastroenterol Hepatol. 2002; 17(Suppl):S85–S104. [PubMed: 12000596]
37. DaCosta RS, Wilson BC, Marcon NE. Optical techniques for the endoscopic detection of dysplastic colonic lesions. Curr Opin Gastroenterol. 2005; 21:70–79. [PubMed: 15687888]
38. Inomata H, Tamai N, Aihara H, et al. Efficacy of a novel autofluorescence imaging system with computer-assisted color analysis for assessment of colorectal lesions. World J Gastroenterol. 2013; 19:7146–7153. [PubMed: 24222959]
39. Singh R, Jayanna M, Navadgi S, et al. Narrow-band imaging with dual focus magnification in differentiating colorectal neoplasia. Dig Endosc. 2013; 25(Suppl 2):16–20. [PubMed: 23617643]
40. Urquhart P, DaCosta R, Marcon N. Endoscopic mucosal imaging of gastrointestinal neoplasia in 2013. Curr Gastroenterol Rep. 2013; 15:330. [PubMed: 23771504]
41. Zavaleta CL, Garai E, Liu JT, et al. A Raman-based endoscopic strategy for multiplexed molecular imaging. Proc Natl Acad Sci U S A. 2013; 110:E2288–E2297. [PubMed: 23703909]
42. Muguruma N, Miyamoto H, Okahisa T, Takayama T. Endoscopic molecular imaging: status and future perspective. Clin Endosc. 2013; 46:603–610. [PubMed: 24340252]
43. Fisher LR, Hasler WL. New vision in video capsule endoscopy: current status and future directions. Nat Rev Gastroenterol Hepatol. 2012; 9:392–405. [PubMed: 22565098]
44. Chu X, Poh CK, Li L, et al. Epitomized summarization of wireless capsule endoscopic videos for efficient visualization. Med Image Comput Comput Assist Interv. 2010; 13:522–529. [PubMed: 20879355]
45. Hsiung PL, Hardy J, Friedland S, et al. Detection of colonic dysplasia in vivo using a targeted heptapeptide and confocal microendoscopy. Nat Med. 2008; 14:454–458. [PubMed: 18345013]
46. Uddin MJ, Crews BC, Blobaum AL, et al. Selective visualization of cyclooxygenase-2 in inflammation and cancer by targeted fluorescent imaging agents. Cancer Res. 2010; 70:3618–3627. [PubMed: 20430759]
47. Segal E, Prestwood TR, van der Linden WA, et al. Detection of intestinal cancer by local, topical application of a quenched fluorescence probe for cysteine cathepsins. Chem Biol. 2015; 22:148–158. [PubMed: 25579207]
48. Goetz M, Ziebart A, Foersch S, et al. In vivo molecular imaging of colorectal cancer with confocal endomicroscopy by targeting epidermal growth factor receptor. Gastroenterology. 2010; 138:435–446. [PubMed: 19852961]
49. Ginty F, Adak S, Can A, et al. The relative distribution of membranous and cytoplasmic met is a prognostic indicator in stage I and II colon cancer. Clin Cancer Res. 2008; 14:3814–3822. [PubMed: 18559601]

50. Wielenga VJ, van der Voort R, Taher TE, et al. Expression of c-Met and heparan-sulfate proteoglycan forms of CD44 in colorectal cancer. Am J Pathol. 2000; 157:1563–1573. [PubMed: 11073815]

51. Ellis LM, Takahashi Y, Liu W, Shaheen RM. Vascular endothelial growth factor in human colon cancer: biology and therapeutic implications. Oncologist. 2000; 5(Suppl 1):11–15. [PubMed: 10804085]

52. Togashi K, Hewett DG, Whitaker DA, Hume GE, Francis L, Appleyard MN. The use of acetic acid in magnification chromocolonoscopy for pit pattern analysis of small polyps. Endoscopy. 2006; 38:613–616. [PubMed: 16612744]

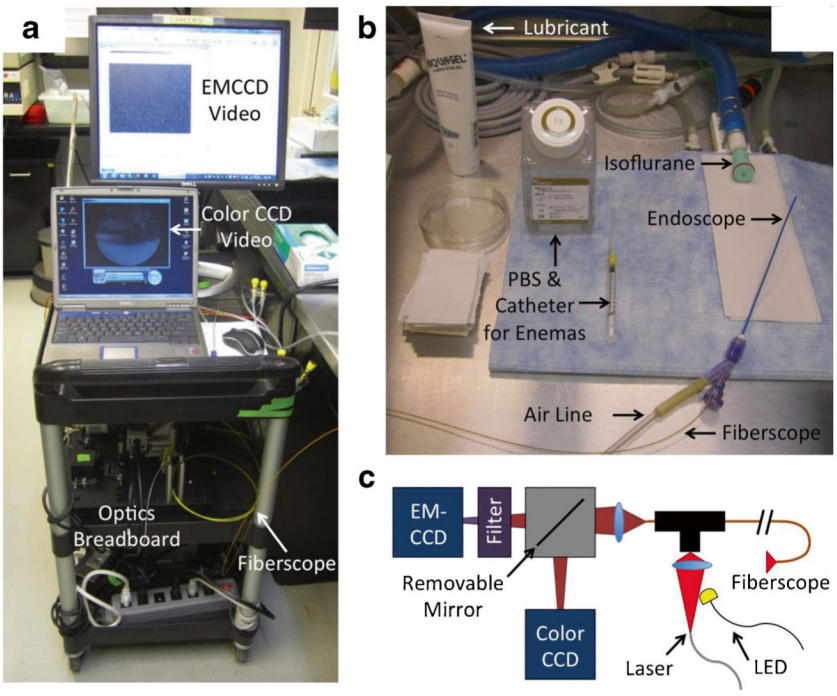

Fig. 1.

a Cart system containing optics, computers, and air pump. **b** Small animal fluorescence endoscope, consisting of 1.8-mm diameter thin-wall plastic tubing glued to a Y connector used to introduce the fiberscope and airflow into the colon. **c** Schematic of optics breadboard. The detection system consists of a sensitive EMCCD camera and color CCD camera switched via a removable mirror. Illumination from either a 660-nm laser or white-light LED (electronically switched) is coupled through the fiberscope.

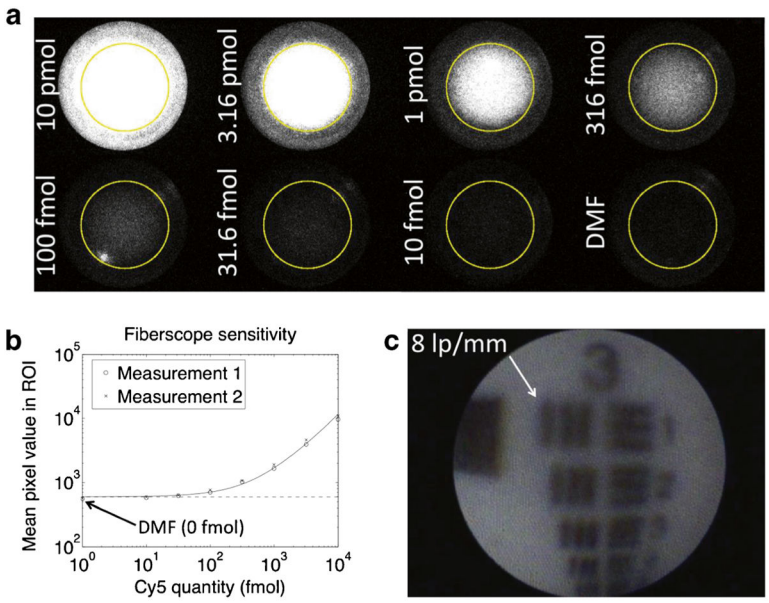

Fig. 2.

Fiberscope fluorescence sensitivity and white-light resolution tests. **a** Fluorescence images of Cy5 dilutions in wells. Images are contrast scaled equally for visualization but not quantitation. **b** Average fluorescence signals within ROIs. **c** White-light image of 1951 USAF resolution test pattern showing the fiberscope's ability to resolve eight line pairs/millimeter (62.5 μm line thickness).

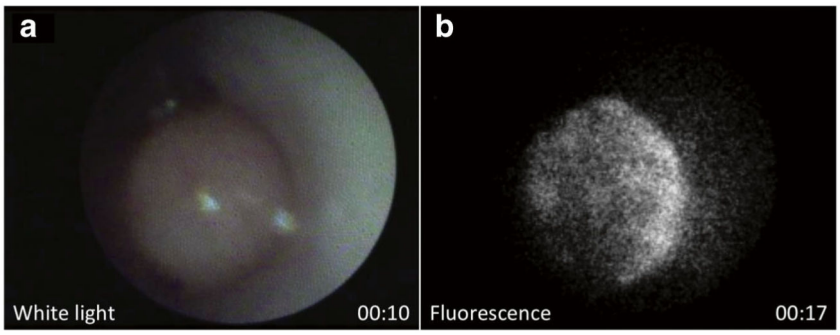

Fig. 3.

In vivo white-light and fluorescence imaging of colon polyp after treatment with BMV109. **a** White-light frame from Video 1, taken at 10-s time point. **b** Fluorescence frame from Video 1, taken at 17-s time point after removing mirror and switching illumination from LED to 660 nm laser. (Video 1, MOV, 8.1 MB).

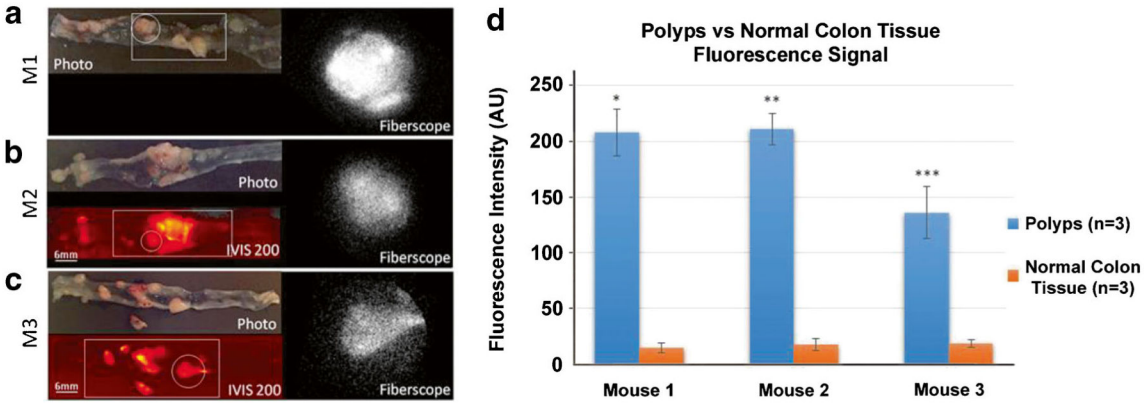

Fig. 4.

Wide-field images of excised mouse colon tissue, after treatment with BMV109 cathepsin-targeting fluorescent probe, using various modalities. **a** Photo (*top left*) and single frame from fluorescence fiberscope (*right*, Video 2) of a colon tissue from mouse M1 (IVIS 200 image not taken for mouse 1). The *white circle* and *square* in the photo indicate the displayed fiberscope frame and approximate field of view surveyed in the video clip, respectively. **b** Photo (*top left*), IVIS 200 fluorescence image (*bottom left*), and fluorescence fiberscope frame (*right*, Video 3) of a tissue from mouse M2. **c** Same as **b** but an excised tissue from mouse M3 (fiberscope frame on *right* from Video 4). **d** Graph depicting significant differences between fluorescence signal intensity between colon polyps and normal adjacent tissue from images acquired with our newly developed fiberscope (*one asterisk* indicates $p = 0.0004$) (*two asterisks* indicate $p = 0.0001$) (*three asterisks* indicate $p = 0.004$) (AU signifies arbitrary units). The values reported appear as mean ± standard error of mean (SEM). (Videos 2–4, MOV, 1.6, 7.1, 7.8 MB).

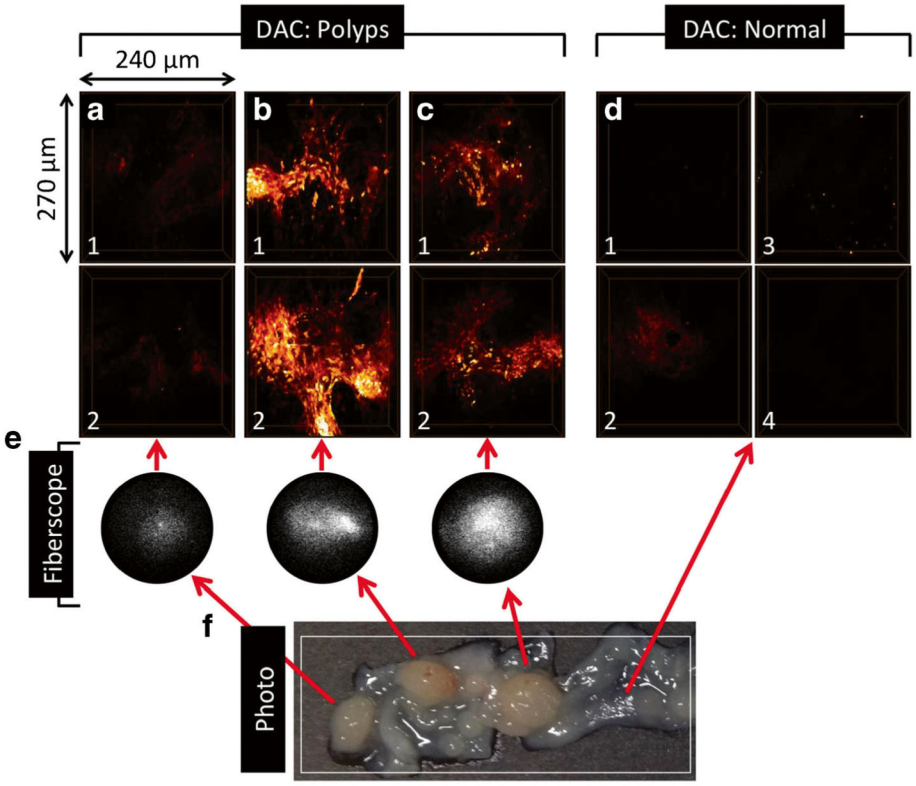

Fig. 5.

a–d Dual-axis confocal volumetric images of excised colon tissue from a mouse treated with BMV109. **a–c** are polyps (two images acquired from each), and **d** are randomly selected surrounding normal mucosa (four images). Approximate dimensions are 240 (width) × 270 (height) × 64 (depth) μm^3. **e** Fluorescence fiberscope frames from Video 5 showing BMV109 contrast in tumors compared to surrounding normal. **f** Photo showing tissue prior to polyp excision. *Red arrows* link polyps in the photo to corresponding fiberscope and DAC microscope images. *White box* shows approximate field of view surveyed in Video 5. (Video 5, MOV, 4.6 MB).